



## Co-influence of the pore size of adsorbents and the structure of adsorbates on adsorption of dyes

Dandan Li<sup>a,c</sup>, Jiaqi Li<sup>a</sup>, Qingbao Gu<sup>b</sup>, Shaoxian Song<sup>d</sup>, Changsheng Peng<sup>a,b,\*</sup>

<sup>a</sup>The Key Lab of Marine Environmental Science and Ecology, Ministry of Education, Ocean University of China, Qingdao 266100, China, Tel./Fax: +86 53266782011; email: [cspeng@ouc.edu.cn](mailto:cspeng@ouc.edu.cn) (C. Peng)

<sup>b</sup>State Key Laboratory of Environmental Criteria and Risk Assessment, Chinese Research Academy of Environmental Sciences, Beijing 100012, China

<sup>c</sup>Qingdao Sun and Ocean Energy Conservation and Environmental Protection Co., Ltd, Qingdao 266108, China

<sup>d</sup>School of Resources and Environmental Engineering, Wuhan University of Technology, Wuhan 430070, China

Received 30 January 2015; Accepted 17 June 2015

### ABSTRACT

To investigate the co-influence of the pore size of adsorbents and the structure of adsorbates on adsorption capacity and rate, the adsorption of basic dyes, methylene blue (MB), and crystal violet (CV) onto a granular adsorbent based on fly ash (GAF) and a granular activated carbon (GAC) were conducted. MB and CV were selected as the target adsorbates due to their similar molecular weights (MB: 319.85 g/mol and CV: 407.98 g/mol) but different molecular structures (MB is line-shaped and CV is fork-shaped). Two different kinds of adsorbents, GAF and GAC, were used here: GAF, a mesoporous adsorbent (average pore diameter  $\approx$  4.28 nm) with small surface area (21.94 m<sup>2</sup>/g), and GAC, a microporous adsorbent (average pore diameter  $\approx$  0.45 nm) with high surface area (1,306 m<sup>2</sup>/g). Although the surface area of GAC was almost 60 times of GAF, the results of adsorption showed the adsorption capacity of GAC for MB was only 1.5 times of GAF (354.59 mg/g of GAC and 262.58 mg/g of GAF), whereas the adsorption capacity of GAC for CV was even less than that of GAC (327.77 mg/g of GAC and 430.73 mg/g of GAF). Moreover, the  $k_p$  values obtained from intra-particle diffusion theory showed that the adsorption rate of both MB and CV in GAF were far bigger than in GAC. Thus, when choosing an adsorbent, surface area is not only the parameter should be considered, the pore size of adsorbents and the structure of adsorbates should also be considered.

*Keywords:* Pore size; Adsorbate structure; Adsorption capacity; Methylene blue; Crystal violet

### 1. Introduction

Synthetic dyes, which have developed fast and replaced the position of natural dyes since twentieth century, have been widely used not only in textile printing and dyeing, but also papermaking, plastics,

leather, rubber, coatings, printing ink, cosmetics, photographic materials, and so on [1,2]. However, since reactive dyes are characterized by high solubility in water, and low rates of fixation, large amounts of effluent from textile industry pose great threat to the environment, which in turn draws widespread attention [3–5]. In China, synthetic dyes have a high

\*Corresponding author.

content of organic compounds (1,000–100,000 mg/L) and high colority (500–500,000 bold) and have caused severe pollution.

Adsorption has received considerable attention for its advantages of removing varieties of dyes, producing high-quality treated water and simplifying the operation procedures [6,7]. Generally, activated carbon (CV) is widely used due to its high surface area and abundant pores. For instance, an AC obtained from flamboyant pods, which possessed a high surface area (1479 m<sup>2</sup>/g) with a considerable amount of mesopores (~50%), had shown an adsorption capacity of 643 mg/g for the adsorption of food yellow 4 (1.17 cm<sup>3</sup>/g) [8]. Similarly, a cobalt nanoparticle-embedded magnetic-ordered mesoporous carbon with a high surface area of 955.3 m<sup>2</sup>/g and an average pore size of 4.3nm was used to removal of T-shaped rhodamine B and reached an equilibrium adsorption capacity of 468 mg/g [9]. Surface area and mesopores seemed to play an important role in adsorption of dyes. However, a microporous carbon felt with a high surface area (1,405 m<sup>2</sup>/g) and a large number of pores below 1nm was applied on adsorption of dyes, and the equilibrium capacities were only 220 mg/g for AR42 (1.27 nm × 0.88 nm × 0.58 nm) and 21 mg/g for RB5 (1.73 nm × 1.5 nm × 0.42 nm) [10]. Micropores limit the diffusion of large molecules and thus decreased the availability of high surface area for activated site adsorption [11]. The pore size of adsorbents is considered to be an important role in determining adsorption capacity [12–16]. Meanwhile, some studies focused on the influence of molecular structure on adsorption per-

formance [17,18]. Malarvizhi and Ho [17] prepared an AC for adsorption of dyes (MB, CV) and the results showed that the adsorption capacity of MB was higher than that of CV, which was attributed to the difference between the molecular structure. However, the co-influence of the pore size of adsorbents and the structure of adsorbates in determining the adsorption capacity and rate has not been broadly studied.

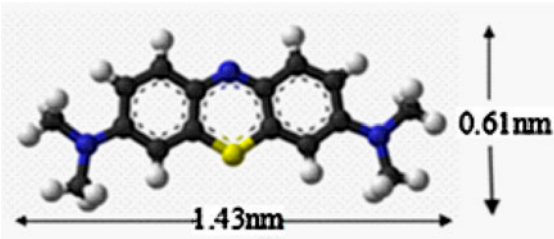
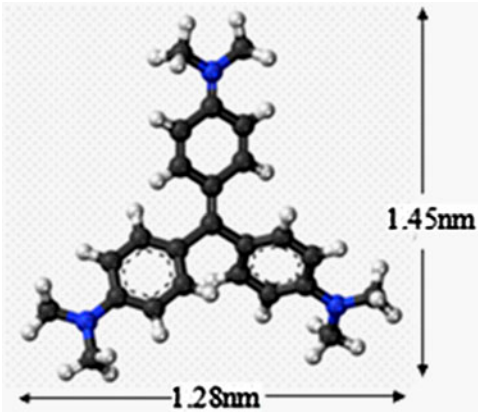
The goal of the present work was to investigate the importance of the pore size of adsorbents and the structure of adsorbates on adsorption performance. A mesoporous adsorbent with small surface area called granular adsorbent based on fly ash (GAF) and a microporous with high surface area called granular activated carbon (GAC) were prepared for adsorption of dyes (methylene blue (MB), crystal violet (CV)) at different initial concentrations. MB and CV were chosen as the target adsorbates because both the dyes are widely used in industries and belong to the same family-basic dyes, while exhibit different molecular structure [19]. Intra-particle diffusion theory was applied to research on the adsorption rate of both dyes by GAF and GAC.

## 2. Materials and methods

### 2.1. Adsorbates

MB and CV were selected as targeted adsorbates for adsorption because they are widely used and cause severe pollution. Moreover, they belong to the same group of basic dyes but have different molecular size and structure. The characteristics of the dyes are listed

Table 1  
Physical and chemical properties of MB and CV

Properties	MB	CV
Chemical formula	C <sub>16</sub> H <sub>18</sub> ClN <sub>3</sub> S	C <sub>25</sub> H <sub>30</sub> ClN <sub>3</sub>
Molecular weight	319.85 (g/mol)	407.98 (g/mol)
Dye nature	Basic	Basic
Molecular size	1.43 nm × 0.61 nm × 0.4 nm	1.45 nm × 1.28 nm × 0.35 nm
Molecular structure		

in Table 1. Both MB and CV used are analytically pure and were produced from Sinopharm and Tianjin Damao, respectively. As shown, MB molecular can be classified as a line-shaped structure while CV shows a fork-shaped structure [20,21]. When subjected to different kinds of adsorbents, they behave differently. Therefore, MB and CV were chosen for this research.

## 2.2. Adsorbents

A mesoporous adsorbent called GAF and a microporous adsorbent called GAC were prepared to

investigate the influence of pore size of adsorbents on adsorption. In this study, GAC was purchased from Shenhua ningxia coal industry group and no further treatment for it was made. GAF was prepared in laboratory, and the following procedure was used to prepare GAF. Fly ash, attapulgite, and starch were mixed evenly in the mass proportion of 6:4:3 and compressed into a model of elongated cylinder-type bottle. The materials were then dried in air and the electro-thermostatic blast oven, respectively, for 24 h, after which the granules were calcined in an atmosphere sintering furnace at a heating rate of 1°C/min and soaked at 600°C for 1 h.

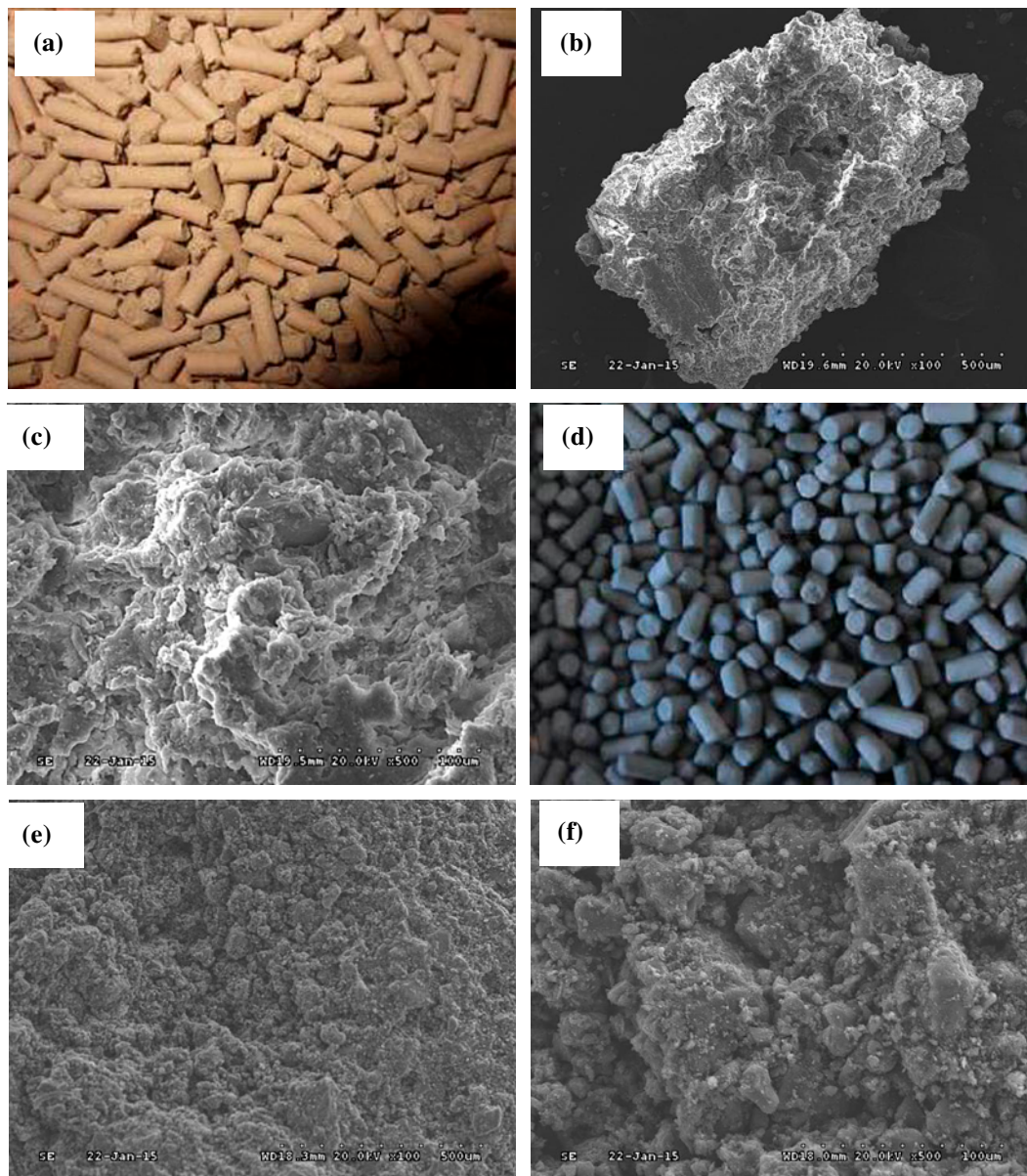


Fig. 1. (a–c) Original photo and SEM images of GAF, (d–f) original photo, and SEM images of GAC.

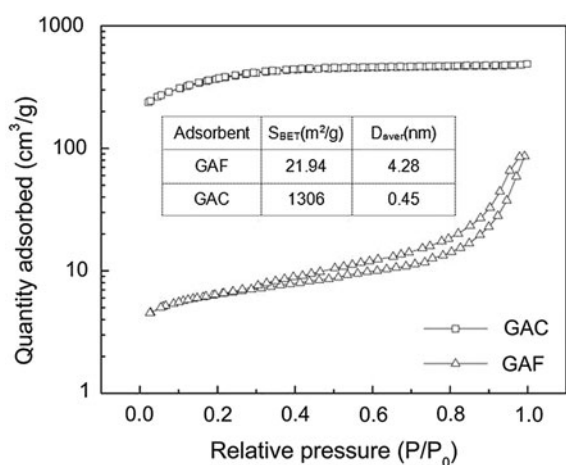


Fig. 2. Adsorption and desorption isotherms of nitrogen on GAC and GAF.

To have a clear observation of GAF and GAC surface properties, scanning electron microscopy (JSM-6700F) was used to make an observation of the adsorbents. The original and SEM images of GAC and GAF were represented in Fig. 1(a–f). The particle size of GAF was about 5–10 mm in length and 3 mm in diameter, while the size of GAC was about 3–5 mm in length and 3 mm in diameter. From the SEM images, it can be seen that both the surface of GAF and GAC were filled with abundant but irregular pores.

To have a deep research about the structure of the adsorbents, nitrogen gas adsorption–desorption at 77 K (Quantachrome Autosorb 1) was performed. The specific surface area of the adsorbents was calculated by BET method, and the pore size distribution was calculated by BJH method. Fig. 2 shows the adsorption and desorption isotherm of nitrogen on GAC and GAF at 77 K. According to IUPAC classification, the isotherm of nitrogen on GAC belongs to type I, Langmuir adsorption isotherm, indicating the development of micropores [22]. As for GAF, it can be classified as

type IV [23]. From Fig. 2, it can be observed that when the relative pressure is less than 0.4, monolayer adsorption happens; while when the relative pressure is greater than 0.4, the isotherm rises fast and an apparent adsorption–desorption loop occurs, indicating the existence of mesopores. The BET surface area ( $S_{BET}$ ) and average diameter ( $D_{aver}$ ) figures are listed in a table among Fig. 2. It can easily be observed that the surface area of GAC is 1,306  $m^2/g$ , nearly 60 times of GAF (21.94  $m^2/g$ ), while the average pore diameter of GAC is 0.45 nm, only one tenth of GAF (4.28 nm). Even though it is undeniable that some pores with size bigger than 0.45 nm exist in GAC, it must be admitted that such slit-shaped micropores seem not to be suitable for adsorbing large-scale dye molecules.

Chemical properties of the adsorbents were also rather important for adsorption. The pH of point of zero charge ( $pH_{ZPC}$ ) of GAF and GAC was determined by Zeta potential instrument (ZS90, Malven). 0.25 mol/L HCl and 0.25 mol/L NaOH were prepared to adjust the pH values of the powder adsorbents solutions to 2, 3, 4, 5, 6, 7, and 8. As shown in Fig. 3(a) and (b), the plots of Zeta potential  $q_t$  pH indicated that the  $pH_{ZPC}$  of GAF and GAC was 1.5 and 3.0, respectively.

### 2.3. Adsorption method

The solutions of MB and CV with different initial concentrations (200, 600, 1,000, 1,200, 1,600, 2,000, 2,500, and 3,000 mg/L) were prepared by mixing some dry powder with distilled water. The adsorption experiments were carried out by mixing 100 mL of dye solution with 0.5000 g adsorbents in conical flasks of 250 mL. The flasks were shaken in a shaker with a constant speed of 120 rpm and temperature of 50°C. At the certain time (2, 6, 18, 22, 28, 40, 46, 70, 94, 118, 142, and 166 h), 0.5 mL solutions were sampled and filtered through a 0.45- $\mu m$  syringe filter and then ana-

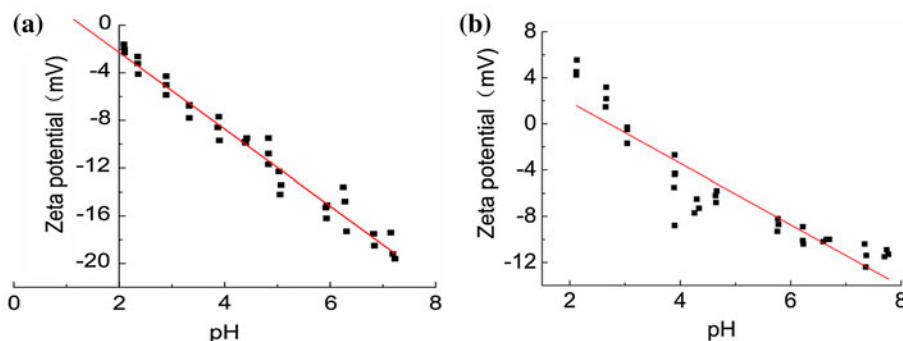


Fig. 3. Zeta potential of (a) GAF and (b) GAC at different pH values.

lyzed by UV spectrophotometer at the maximum absorption wavelength of 665 nm for MB and 583 nm for CV to estimate the residual dye concentration. The equilibrium adsorption capacity at different dye concentration was calculated as follows:

$$q_e = \frac{(C_0 - C_e)V}{m} \quad (1)$$

where  $C_0$  (mg/L) is the initial concentration,  $C_e$  (mg/L) is the equilibrium concentration,  $V$  (L) is the volume of the dye, and  $m$  (g) is the weight of the adsorbent.

### 3. Results and discussion

#### 3.1. Adsorption results of MB and CV

The pictures of initial dye and adsorbed dye by GAF and GAC were shown in Fig. 4. For adsorption of MB, GAC obviously showed more efficiency than GAF, while for adsorption of CV, GAF seemed to be more efficient than GAC. To make a further research of this phenomenon, some liquid-phase experiments were carried out.

Fig. 5 showed the adsorption isotherms of MB and CV on GAC and GAF. To show the adsorption behavior more clearly, trend lines were added in Fig. 5(a) and (b). Since the original pH values of MB and CV with concentration from 200 to 3,000 mg/L were between 4 and 6.5, while the  $\text{pH}_{\text{ZPC}}$  of GAF and GAC was 1.5 and 3.0, respectively, it can be induced that the surfaces of GAF and GAC were both negative and could attract positively charged dyes, MB and CV.

It is evident from Fig. 5(a) that as the initial concentration of MB increased from 200 to 3,000 mg/L, GAC always presented higher adsorption capacity than GAF owe to big surface area. These results showed much

similarly with the adsorption of MB using cross-linked polyaniline and conventional polyaniline [24]. It is clear from Fig. 2 that the surface area of GAC (1,306  $\text{m}^2/\text{g}$ ) is extremely larger than that of GAF (21.94  $\text{m}^2/\text{g}$ ). Assuming that the surface area of GAC is covered completely by dye molecules, the adsorption capacity of GAC should be much higher than that of GAF. However, the fact was that the equilibrium adsorption capacity of MB on GAC (354.59 mg/g) even did not reach twice the amount of MB on GAF (262.58 mg/g). The reason for this phenomenon is mainly due to the incompatible correlation between the pore structure of MB molecules and the pore size of GAC. According to Table 1, the molecule structure of MB shows a line-shaped structure. Therefore, only if the pore size of the adsorbent is larger than the second width of MB molecular, dye molecules can get access to the inner surface and adsorbed onto activated sites. The average diameter of GAF and GAC is shown in Fig. 2, which shows that MB molecules can easily pass through the pores of GAF. As for GAC, its average diameter is 0.45 nm and has some pores bigger or smaller than 0.45 nm, so that only part of pores is available for dye molecules to penetrate. Moreover, the diffusion of adsorbates in the micropores may be intervened by the preadsorbed molecules [25,26]. That is to say, the size of the micropores limits the accessibility to the surface for large molecules like dyes.

As for fork-shaped CV, it can be seen from Fig. 5(b) that GAF exhibited better performance than GAC, which was opposite to the adsorption of MB. It has to be pointed out that mesopores of GAF facilitated the adsorption of CV to some extent. A comparative study on adsorption performances of an activated carbon from waste rubber tire and a commercial activated carbon for acid blue 113 also came to a similar conclusion that larger mesopore volume accounts for a

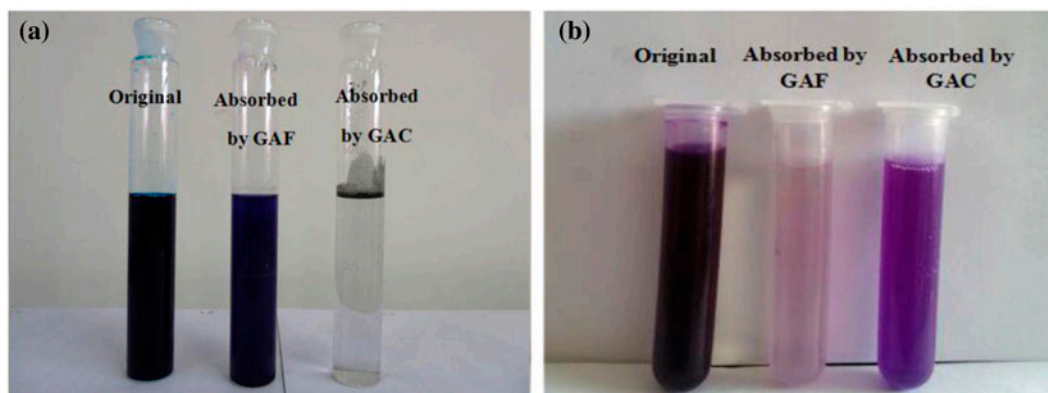


Fig. 4. Photographs of original dyes and dyes adsorbed by GAF and GAC: (a) MB and (b) CV.

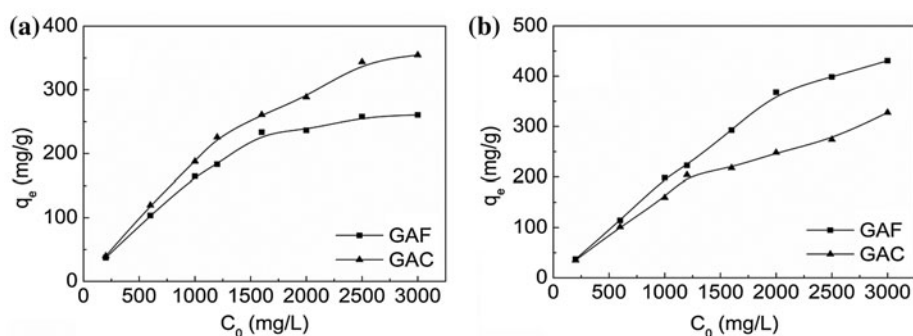


Fig. 5. Adsorption isotherms of dyes on GAF and GAC: (a) MB and (b) CV.

higher adsorption capacity although the commercial carbon has a higher micropore volume and a higher surface area [27]. From Fig. 2, it can be observed that GAF contains abundant mesopores while GAC only consists of micropores. Moreover, the structure of CV is fork-shaped and has a molecular size of  $1.45 \text{ nm} \times 1.28 \text{ nm} \times 0.35 \text{ nm}$ , showing that it is obviously bigger than the pore width of GAC. This suggests that the cross-sectional area of some throats in micropores is too small for the adsorbates to penetrate and thus hold back activated sites adsorption [28,29]. Compared to GAC, GAF provides wide channels for CV molecules due to mesopores and enables adsorbates to be adsorbed on its surface. With existence of mesopores, adsorbates can pass through the diffusion path smoothly and thus cover a large portion of inner surface of adsorbent. As a consequence, in case of dye molecules, the correlation between the pore size of adsorbents and the structure of adsorbates make more contribution than surface area in determining the adsorption capacity.

### 3.2. Adsorption isotherm models

To understand the mechanisms of adsorption, three commonly used types of isothermal models, Langmuir, Freundlich, and Tempkin model [30], were employed to describe the adsorption of MB and GV on GAC and GAF.

The Langmuir isotherm assumes that the surface of the solid is homogeneous and one specific site within the adsorbent can only match a molecular without access of others. When the isotherm reaches a plateau, it indicates that adsorption occurs no more and equilibrium has appeared. The Langmuir linear equation can be expressed as:

$$\frac{C_e}{q_e} = \frac{1}{bq_m} + \frac{C_e}{q_m} \quad (2)$$

of which  $q_e$  is the amount of dye adsorbed on the adsorbent surface at equilibrium and  $C_e$  is the concentration of the adsorbate at equilibrium, while  $q_m$  and  $b$  are the behalf of maximum adsorption capacity and Langmuir constant, respectively. Furthermore, another constant called  $R_L$  can be deduced by the equation as follows:

$$R_L = \frac{1}{1 + bC_0} \quad (3)$$

where  $C_0$  is the initial concentration of dye. When the value of  $R_L$  is between 0 and 1, it indicates that the adsorption is favorable, otherwise, unfavorable.

The Freundlich isotherm, as an empirical model, describes the process of multilayer adsorption on uneven solid surfaces and is given by the following equation.

$$\log q_e = \log K_f + \frac{1}{n} \log C_e \quad (4)$$

As listed above,  $q_e$  and  $C_e$  represent the amount of adsorbed dye on the adsorbent and the concentration of the dye at equilibrium, respectively.  $K_f$  and  $n$ , the constants of the model, indicate the adsorption capacity of the adsorbent and the intensity of adsorption. The value of  $K_f$  higher, the adsorption capacity is better. Moreover, if the value of  $1/n$  exits between 0.1 and 0.5, it indicates the adsorption is favorable. However, it becomes difficult for adsorption when the value of  $1/n$  is greater than 2.

The Tempkin isotherm, at the earliest, was used to describe the adsorption process of hydrogen on platinum electrode in the acid solution. It is the characteristic of considering the interaction between the adsorbate and adsorbent, such as electrostatic attrac-

tion and ion exchange. The model can be expressed as follows:

$$q_e = B_t \ln A_t + B_t \ln C_e \quad (5)$$

where  $B_t$  and  $A_t$  are constants of the Temkin isotherm.

The relevant parameters of three isotherms are listed in Table 2. Since the  $R^2$  values of the Langmuir model are all higher than those of the Freundlich model and the Temkin model, it can be concluded that the Langmuir model fits better than the other models for the adsorption data of two dyes on GAF and GAC. Thus, the process of the adsorption belongs to monolayer coverage, indicating that once a molecular occupies an adsorbent site, none of others can be adsorbed on it again. In addition, the  $R_L$  values of the Langmuir model range from 0 to 1, and the values of  $1/n$  are between 0.1 and 0.5, proving that the adsorption is favorable. As shown in the Langmuir model, the maximum adsorption capacities for MB onto GAF and GAC were 277.78 and 357.14 mg/g, respectively, while for CV onto GAF and GAC were 476.19 and 347.15 mg/g, respectively. The results were in agreement with Fig. 5 and thus proved the importance of adsorbents and adsorbates properties on adsorption in return.

### 3.3. Adsorption kinetics

To quantitatively explain the effect of pore size and adsorbate structure on adsorption capacity, further kinetic studies and data interpretation were conducted in this section.

The adsorption kinetics of dyes (MB and CV) with initial concentrations (600, 1,000 mg/L) onto GAF and GAC were shown in Figs. 6 and 7. To clearly show

the trend of adsorption process, smooth curves were added in Figs. 6 and 7. As can be seen from Fig. 6, the adsorption trend of MB on GAF and GAC were almost the same. The adsorption capacity of MB (600, 1,000 mg/L) on GAF and GAC both rose rapidly in the first few hours and then the adsorption process rate gradually slowed down and finally reached equilibrium at 72 h for MB (600 mg/L) and 118 h for MB (1,000 mg/L). However, it can be seen from Fig. 7 that GAF presented an extremely fast adsorption speed for CV (600 mg/L, 1,000 mg/L) and reached equilibrium at approximately 28 h for CV (600 mg/L) and 40 h for CV (1,000 mg/L). On the contrary, the adsorption process of CV (600 mg/L, 1,000 mg/L) by GAC went on slowly and reached equilibrium at about 144 h.

To explain this phenomenon, the following studies were made.

According to Webber and Morris, the intra-particle diffusion controls the rate of adsorption process and the step from liquid to adsorbent surface can be neglected. The equation is as follows:

$$q_t = k_p t^{1/2} + C \quad (6)$$

where  $k_p$  is the intra-particle diffusion rate constant, and  $C$  is the value of the intercept of the plot of  $q_t$  against  $t^{1/2}$ .

According to the equation above, the plot of  $q_t$  vs.  $t$  should go through the origin if the intra-particle diffusion is the only rate-limiting step [31]. However, as can be seen from Fig. 8, the diffusion process can be classified into three phases, showing that intra-particle diffusion is not the single rate-limiting step in the adsorption of MB and CV. The first phase is an instantaneous adsorption and is probably due to a strong electrostatic attraction between the adsorbate and the outer surface of the adsorbent. The second

Table 2  
Parameters of the adsorption isotherm models for MB and CV on GAF and GAC

Parameters items		MB on GAF	MB on GAC	CV on GAF	CV on GAC
Langmuir	$q_m$ (mg/g)	277.78	357.14	476.19	347.15
	$b$	0.0083	0.0209	0.0116	0.0041
	$R^2$	0.9982	0.9883	0.9778	0.9725
	$R_L$	0.03–0.37	0.01–0.19	0.02–0.31	0.07–0.54
Freundlich	$K_f$ (mg/g)	16.14	62.14	35.50	9.57
	$1/n$	0.4059	0.2572	0.3954	0.5018
	$R^2$	0.9224	0.8848	0.5982	0.8790
Temkin	$b_T$	50.11	40.08	77.79	67.48
	$A_T$	0.1397	3.6282	0.3154	0.0624
	$R^2$	0.9698	0.9571	0.7987	0.9440

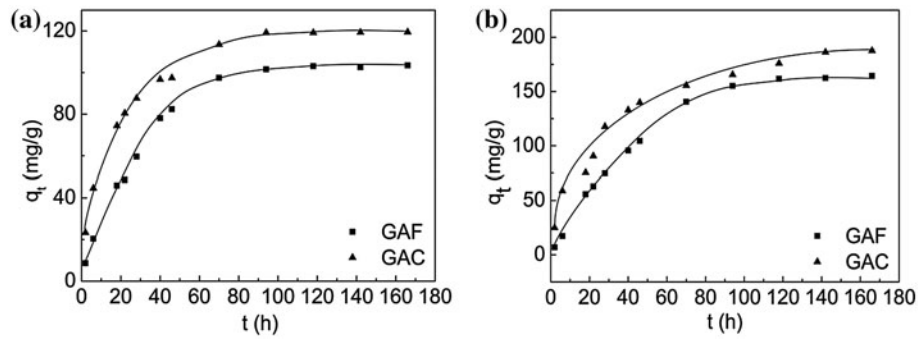


Fig. 6. Adsorption kinetics of MB by GAF and GAC: (a) 600 mg/L and (b) 1,000 mg/L.

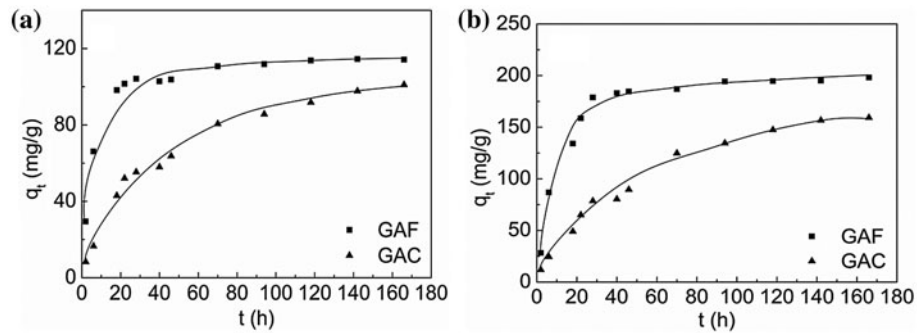


Fig. 7. Adsorption kinetics of CV by GAF and GAC: (a) 600 mg/L and (b) 1,000 mg/L.

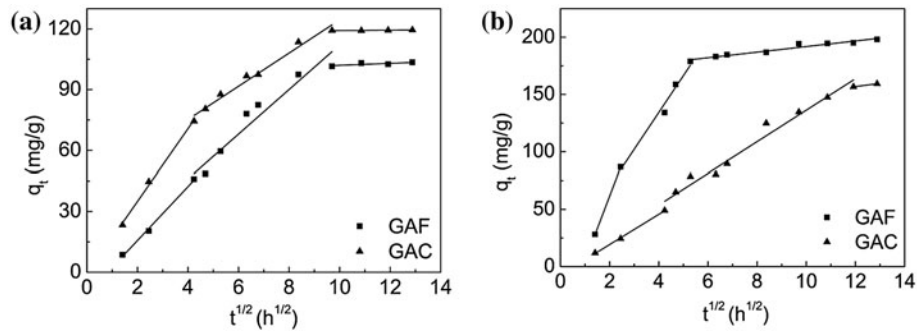


Fig. 8. Intra-particle diffusion model for dyes on GAF and GAC: (a) MB and (b) CV.

phase is a gradual adsorption because of the intra-particle diffusion of dye molecules passing through the pores of the adsorbent. The final phase is equilibrium adsorption when the dye molecules occupy all of the active sites of the adsorbent [32,33]. The values of  $k_p$  were calculated from the slope of corresponding data and were presented in Tables 2 and 3. The intra-particle diffusion model of MB (600 mg/L) and CV (1,000 mg/L) onto GAF and GAC were shown in Fig. 8(a) and (b).

The straight lines with higher slope have higher  $k_p$  values, indicating a higher adsorption rate per unit time. For the adsorption of MB, it can be clearly seen from Table 3 and Fig. 8(a) that as time passed, both the rate of GAF and GAC decreased and the adsorption finally reached equilibrium. During the second stage (intra-particle diffusion), the difference between the  $k_p$  values of GAF and GAC was so small, indicating that the MB molecules can pass through the pores of both GAF and GAC. While from Fig. 8(b), one can

Table 3

Kinetic parameters of intra-particle diffusion model for the adsorption of MB onto GAF and GAC

	GAF			GAC		
	1st stage	2nd stage	3rd stage	1st stage	2nd stage	3rd stage
$k_p$	13.29	11.14	0.27	17.90	8.28	0.09
C	-10.91	1.29	100.01	-0.86	42.82	118.25
$R^2$	0.9936	0.9382	0.9147	0.9935	0.9603	0.5107

Table 4

Kinetic parameters of intra-particle diffusion model for the adsorption of CV onto GAF and GAC

	GAF			GAC		
	1st stage	2nd stage	3rd stage	1st stage	2nd stage	3rd stage
$k_p$	56.36	32.16	2.11	13.19	13.74	2.76
C	-51.26	5.60	169.75	-7.13	-1.19	123.74
$R^2$	-	0.9740	0.8604	0.9978	0.9701	-

see that the adsorption process of CV onto GAF was much faster than GAC. In addition, as can be seen from Table 4, the intra-particle diffusion  $k_p$  value of GAF is much higher than that of GAC, indicating that it is easier for CV molecules pass through the pores of GAF than that of GAC. This can be attributed to the fact that the pores of GAC are not big enough to let big molecules of CV to pass through smoothly. Therefore, from the kinetic studies of MB and CV onto GAF and GAC, it can be concluded that the structure of adsorbates and the pore size of adsorbents have significant effects on the adsorption rate and capacity.

#### 4. Conclusions

The present work has investigated the influence of surface area, the pore size of adsorbents and the structure of adsorbates in determining the adsorption capacity of dyes in aqueous solution. The adsorption results of MB and CV onto GAF and GAC revealed that effective surface area can be decreased since micropores limited the diffusion of molecules and thus caused pore blockage. On the other hand, although MB and CV have similar molecular weight, their molecular structures are quite different from each other. It seems that fork-shaped CV has more difficulty to penetrate into narrow pores of adsorbents than line-shaped MB. Only when the pore of adsorbents is big enough to let adsorbates pass through, more adsorbates can be adsorbed onto activated sites. Moreover, the  $k_p$  values obtained from the intra-particle diffusion theory showed that both adsorption

rate of MB and CV in GAF was higher than GAC. Thus, when choosing an adsorbent, surface area is not only the parameter should be considered, the pore size of adsorbents and the structure of adsorbates should also be considered.

#### Acknowledgments

This work was supported by the State Key Laboratory of Environmental Criteria and Risk Assessment (No. SKLECRA2013OFP12) and the Public science and technology research funds projects of ocean, China (201105020).

#### References

- [1] A. Mittal, J. Mittal, A. Malviya, D. Kaur, V.K. Gupta, Adsorption of hazardous dye crystal violet from wastewater by waste materials, *J. Colloid Interface Sci.* 343 (2010) 463–473.
- [2] G. Zhang, L. Yi, H. Deng, P. Sun, Dyes adsorption using a synthetic carboxymethyl cellulose-acrylic acid adsorbent, *J. Environ. Sci.* 26 (2014) 1203–1211.
- [3] A.W.M. Ip, J.P. Barford, G. McKay, Reactive Black dye adsorption/desorption onto different adsorbents: Effect of salt, surface chemistry, pore size and surface area, *J. Colloid Interface Sci.* 337 (2009) 32–38.
- [4] K.V. Kumar, V. Ramamurthi, S. Sivanesan, Modeling the mechanism involved during the sorption of methylene blue onto fly ash, *J. Colloid Interface Sci.* 284 (2005) 14–21.
- [5] G.O. El-Sayed, Removal of methylene blue and crystal violet from aqueous solutions by palm kernel fiber, *Desalination* 272 (2011) 225–232.

- [6] J. Zolgharnein, M. Bagtash, T. Shariatmanesh, Simultaneous removal of binary mixture of Brilliant Green and Crystal Violet using derivative spectrophotometric determination, multivariate optimization and adsorption characterization of dyes on surfactant modified nano- $\gamma$ -alumina, *Spectrochim. Acta, Part A* 137 (2015) 1016–1028.
- [7] G. Crini, Non-conventional low-cost adsorbents for dye removal: A review, *Bioresour. Technol.* 97 (2006) 1061–1085.
- [8] G. Durán-Jiménez, V. Hernández-Montoya, M.A. Montes-Morán, A. Bonilla-Petriciolet, N.A. Rangel-Vázquez, Adsorption of dyes with different molecular properties on activated carbons prepared from lignocellulosic wastes by Taguchi method, *Microporous Mesoporous Mater.* 199 (2014) 99–107.
- [9] L. Tang, Y. Cai, G. Yang, Y. Liu, G. Zeng, Y. Zhou, S. Li, J. Wang, S. Zhang, Y. Fang, Y. He, Cobalt nanoparticles-embedded magnetic ordered mesoporous carbon for highly effective adsorption of rhodamine B, *Appl. Surf. Sci.* 314 (2014) 746–753.
- [10] L. Donnaperma, L. Duclaux, R. Gadiou, M.P. Hirn, C. Merli, L. Pietrelli, Comparison of adsorption of Remazol Black B and Acidol Red on microporous activated carbon felt, *J. Colloid Interface Sci.* 339 (2009) 275–284.
- [11] W. Tanthapanichakoon, P. Ariyadejwanich, P. Japthong, K. Nakagawa, S.R. Mukai, H. Tamon, Adsorption-desorption characteristics of phenol and reactive dyes from aqueous solution on mesoporous activated carbon prepared from waste tires, *Water Res.* 39 (2005) 1347–1353.
- [12] M. Xia, A. Li, Z. Zhu, Q. Zhou, W. Yang, Factors influencing antibiotics adsorption onto engineered adsorbents, *J. Environ. Sci.* 25 (2013) 1291–1299.
- [13] L.C. Juang, C.C. Wang, C.K. Lee, Adsorption of basic dyes onto MCM-41, *Chemosphere* 64 (2006) 1920–1928.
- [14] Y.R. Lin, H. Teng, Mesoporous carbons from waste tire char and their application in wastewater discoloration, *Microporous Mesoporous Mater.* 54 (2002) 167–174.
- [15] C.T. Hsieh, H. Teng, Influence of mesopore volume and adsorbate size on adsorption capacities of activated carbons in aqueous solutions, *Carbon* 38 (2000) 863–869.
- [16] C.T. Hsieh, H. Teng, Influence of oxygen treatment on electric double-layer capacitance of activated carbon fabrics, *Carbon* 40 (2002) 667–674.
- [17] R. Malarvizhi, Y.S. Ho, The influence of pH and the structure of the dye molecules on adsorption isotherm modeling using activated carbon, *Desalination* 264 (2010) 97–101.
- [18] M.E. Fernandez, G.V. Nunell, P.R. Bonelli, A.L. Cukierman, Activated carbon developed from orange peels: Batch and dynamic competitive adsorption of basic dyes, *Ind. Crops Prod.* 62 (2014) 437–445.
- [19] C.H. Weng, Y.T. Lin, T.W. Tzeng, Removal of methylene blue from aqueous solution by adsorption onto pineapple leaf powder, *J. Hazard. Mater.* 170 (2009) 417–424.
- [20] C. Pelekani, V.L. Snoeyink, Competitive adsorption between atrazine and methylene blue on activated carbon: The importance of pore size distribution, *Carbon* 38 (2000) 1423–1436.
- [21] H. Tamai, T. Yoshida, M. Sasaki, H. Yasuda, Dye adsorption on mesoporous activated carbon fiber obtained from pitch containing yttrium complex, *Carbon* 37 (1999) 983–989.
- [22] R. Wang, X. Cai, F. Shen, TiO<sub>2</sub> hollow microspheres with mesoporous surface: Superior adsorption performance for dye removal, *Appl. Surf. Sci.* 305 (2014) 352–358.
- [23] M. Liu, L.A. Hou, B. Xi, Y. Zhao, X. Xia, Synthesis, characterization, and mercury adsorption properties of hybrid mesoporous aluminosilicate sieve prepared with fly ash, *Appl. Surf. Sci.* 273 (2013) 706–716.
- [24] M. Ayad, S. Zaghlool, Nonastructured crosslinked polyaniline with high surface area: Synthesis, characterization and adsorption for organic dye, *Chem. Eur. J.* 204–206 (2012) 79–86.
- [25] S. Lei, J.I. Miyamoto, H. Kanoh, Y. Nakahigashi, K. Kaneko, Enhancement of the methylene blue adsorption rate for ultramicroporous carbon fiber by addition of mesopores, *Carbon* 44 (2006) 1884–1890.
- [26] J.V. Villarreal Rocha, D. Barrera, K. Sapag, Improvement in the pore size distribution for ordered mesoporous materials with cylindrical and spherical pores using the Kelvin equation, *Top. Catal.* 54 (2011) 121–134.
- [27] V.K. Gupta, B. Gupta, A. Rastogi, S. Agarwal, A. Nayak, A comparative investigation on adsorption performances of mesoporous activated carbon prepared from waste rubber tire and activated carbon for a hazardous azo dye—Acid Blue 113, *J. Hazard. Mater.* 186 (2011) 891–901.
- [28] G. McKay, M.J. Bino, A.R. Altamemi, The adsorption of various pollutants from aqueous solutions on to activated carbon, *Water Res.* 19 (1985) 491–495.
- [29] A. Gil, F.C.C. Assis, S. Albeniz, S.A. Korili, Removal of dyes from wastewaters by adsorption on pillared clays, *Chem. Eur. J.* 168 (2011) 1032–1040.
- [30] K.V. Kumar, Optimum sorption isotherm by linear and non-linear methods for malachite green onto lemon peel, *J. Dyes Pigm.* 74 (2007) 595–597.
- [31] W.T. Tsai, Y.M. Chang, C.W. Lai, C.C. Lo, Adsorption of basic dyes in aqueous solution by clay adsorbent from regenerated bleaching earth, *Appl. Clay. Sci.* 29 (2005) 149–154.
- [32] A. Ahmad, M. Rafatullah, O. Sulaiman, M.H. Ibrahim, R. Hashim, Scavenging behaviour of meranti sawdust in the removal of methylene blue from aqueous solution, *J. Hazard. Mater.* 170 (2009) 357–365.
- [33] K.A.G. Gusmão, L.V.A. Gurgel, T.M.S. Melo, L.F. Gil, Adsorption studies of methylene blue and gentian violet on sugarcane bagasse modified with EDTA dianhydride (EDTAD) in aqueous solutions: Kinetic and equilibrium aspects, *J. Environ. Manage.* 118 (2013) 135–143.